

Two-dimensional structures of adsorbed argon layers

Tung Tsang

*Department of Physics and Astronomy,
Howard University, Washington, D. C. 20059*

(Received 26 March 1979)

The two-dimensional structures of adsorbed argon layers have been described by a modified cell theory with the cell-size variations evaluated by a self-consistent condition. The calculated lattice parameters and the atomic-vibration amplitudes at various temperatures are in satisfactory agreement with neutron scattering data of argon adsorbed on Grafoil substrate. The liquid phase and the melting transition may be absent in the two-dimensional systems. The calculation also indicates a transition between commensurate and incommensurate lattices for argon on Grafoil near 50°K, in agreement with experimental observations.

I. INTRODUCTION

New experimental methods of probing surfaces have greatly increased our knowledge of physical adsorption and of condensed phases of adsorbed gas films.¹⁻⁴ In addition to vapor-pressure isotherms and heat-capacity studies, specific methods for probing surfaces on the atomic scale have also been under intensive development. Many low-energy-electron diffraction (LEED) experiments have established the formation of ordered two-dimensional structures of weakly physisorbed gas layers on many substrates. More recently, direct structural information has been obtained by neutron scattering experiments. For these experiments, a commonly used substrate is Grafoil, an exfoliated graphite foil with large surface areas of exceptional uniformity and homogeneity and with a considerable degree of basal-plane order. By neutron scattering experiments, ordered two-dimensional lattices have been observed⁵⁻⁹ for argon, nitrogen, helium, oxygen, and other gases adsorbed on Grafoil.

In our present work, we have chosen to study the two-dimensional hexagonal lattice¹⁰ of monatomic argon because of the absence of intramolecular degrees of freedom and because of the well-known Lennard-Jones interatomic potential.¹¹ With a self-consistent condition for cell-size variations, a modified cell theory¹² may be used to evaluate the temperature dependences of lattice parameters and vibration amplitudes. The theoretical results may then be compared with the neutron scattering data⁶ of argon on Grafoil because of the smooth substrate potential.¹³ In Sec. II, the modified cell theory will be applied to the two-dimensional hexagonal lattice of argon. We will follow our previous notations¹² in general. In Sec. III, the calculated results are then compared with the neutron scattering experiments⁶ of argon on Grafoil. There appears to be general agreement between the theoretical and the experimental results.

A brief discussion of the results is given in Sec. IV.

The Lennard-Jones interatomic potential $\nu(R)$ for a pair of argon atoms with interatomic distance R is given by

$$\nu(R) = 4\epsilon[(\sigma/R)^{12} - (\sigma/R)^6] \quad (1)$$

where σ and ϵ are the Lennard-Jones diameter and well depth, respectively. For argon, the standard choice^{11,14} is $\sigma = 3.405 \times 10^{-8}$ cm and $\epsilon/k = 120$ °K where k is the Boltzmann constant. Following the standard conventions,¹¹ we will use the mass of an argon atom $m = 6.63 \times 10^{-23}$ g as the mass unit, $\sigma = 3.405 \times 10^{-8}$ cm as the distance unit, and $\epsilon = 1.657 \times 10^{-14}$ erg as the energy unit. In these units, the Lennard-Jones interatomic potential is

$$\nu(R) = 4(R^{-12} - R^{-6}) \quad (2)$$

We will also use the reduced temperature $T^* = kT/\epsilon$ in place of the temperature T . In our units, we may replace kT by T^* .

II. MODIFIED CELL THEORY

For a system of N classical particles, the potential energy of the system is $U(\vec{R}_1, \dots, \vec{R}_N) = \sum \nu_{ij}$, where $\nu_{ij} = \nu(R_{ij})$, $\vec{R}_{ij} = \vec{R}_j - \vec{R}_i$, and the summation is over all ij pairs, $i < j = 1$ to N . The classical partition function Z_N is¹⁵

$$Z_N = (h^2/2\pi mkT)^{-3N/2} Q_N \quad (3)$$

where h is the Planck's constant and Q_N is the configurational integral or configurational partition function

$$Q_N = \int \dots \int e^{-U/T^*} d\vec{R}_1 \dots d\vec{R}_N \quad (4)$$

The Helmholtz free energy A is given by

$$A = -kT \ln Z_N = \frac{3}{2} NkT \ln(h^2/2\pi mkT) + Nf, \quad (5)$$

where f may be regarded as the configurational free energy per particle

$$f = -(T^* \ln Q_N) / N \quad (6)$$

In the modified cell theory,¹² the many-body potential U is approximated by a sum of single-body potentials V

$$U(\bar{\mathbf{R}}_1, \dots, \bar{\mathbf{R}}_N) = \sum_i V_i(\bar{\mathbf{R}}_i) \quad (7)$$

$$V_i = \frac{1}{2} \sum_j v_{ij} = V'_i + V''_i \quad (8)$$

where V'_i is the single-body potential due to the six nearest neighbors (nn) of the two-dimensional hexagonal lattice and V''_i is the potential due to the other neighbors. The subscript i will be omitted and we will write V_i as V .

For a regular two-dimensional hexagonal lattice with nn distance α , the Wigner-Seitz (WS) cell is a regular hexagon with area $\frac{1}{2}(\sqrt{3}\alpha^2)$. The configurational free energy ϕ of the regular lattice is then given by the single-cell partition function Q_1

$$\phi(\alpha) = -T^* \ln Q_1(\alpha) \quad (9)$$

$$Q_1 = \int 2\pi r e^{-V(r)/T^*} dr \quad (10)$$

That is, we will evaluate Q_1 by allowing particle i to move for distance r away from cell center. Since the nearest neighbors are not involved, the potential $V''(r)$ may be approximated¹² by $V''(0)$,

$$2V''(r) = 2V''(0) = 6\nu(\sqrt{3}\alpha) + 6\nu(2\alpha) + 12\nu(\sqrt{7}\alpha) + 6\nu(3\alpha) + \dots \quad (11)$$

with the particles farther away than 3α replaced by a uniform film of density $2/\sqrt{3}\alpha^2$. The nearest-

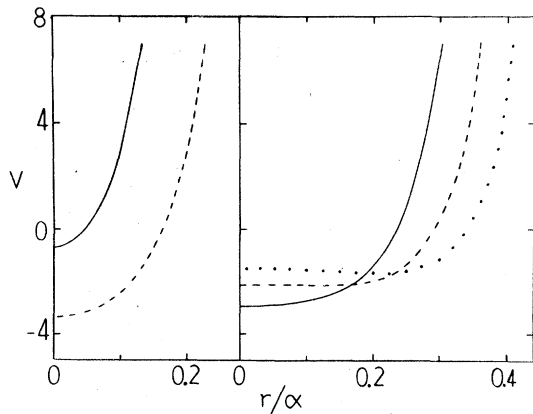


FIG. 1. Cell potential $V(r)$ vs r/α . Left-hand side: solid line, $\alpha = 1.0$; dashed line, $\alpha = 1.1$. Right-hand side: solid line, $\alpha = 1.2$; dashed line, $\alpha = 1.3$; dotted line, $\alpha = 1.4$.

neighbor potential $V'(r)$ is evaluated for displacements along the [10] and [11] axes and then the average value is used, retaining the isotropic part only. The cell potential $V(r) = V'(r) + V''(0)$ is shown in Fig. 1 for several different values of cell parameter α . From $V(r)$, we have evaluated $\phi(\alpha)$ for several temperatures from Eq. (9) and also the canonical average value of r^2

$$\langle r^2 \rangle_\alpha = \int 2\pi r^3 e^{-V/T^*} dr / \int 2\pi r e^{-V/T^*} dr \quad (12)$$

where the angular bracket denotes the canonical average and subscript α denotes the cell size. In Fig. 2, we have shown $\phi(\alpha)$ and the root-mean-square (rms) amplitude $r'(\alpha) = (\langle r^2 \rangle_\alpha)^{1/2}$ for several different temperatures.

Since the structures are not perfectly regular, it is necessary to consider the WS cells as distorted hexagons. The center of the WS cell may be defined as the center of mass of the six nearest neighbors and the cell parameter α may be taken as the average of the six nn distances. The normalized probability distribution $p(\alpha)$ for cell parameter α may be approximated by a Gaussian function with rms deviation α'

$$p(\alpha) = (2\pi\alpha'^2)^{-1/2} \exp[-(\alpha - \alpha_A)^2 / 2\alpha'^2] \quad (13)$$

where $\alpha_A = \int p(\alpha) \alpha d\alpha$ is the average cell parameter.

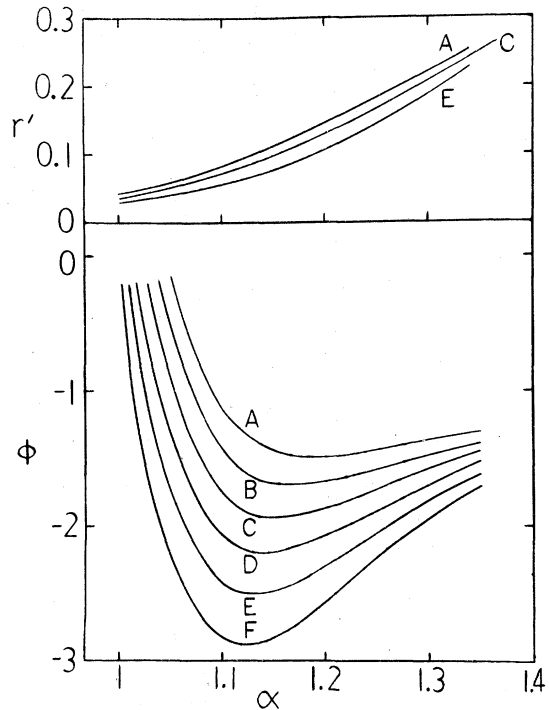


FIG. 2. rms amplitude r' (top diagram) and configurational free energy (lower diagram) vs cell parameter α for fixed cell size. The curves are designated A, B, C, D, E, F for $T^* = 0.6, 0.5, 0.4, 0.3, 0.2$, and 0.1 , respectively.

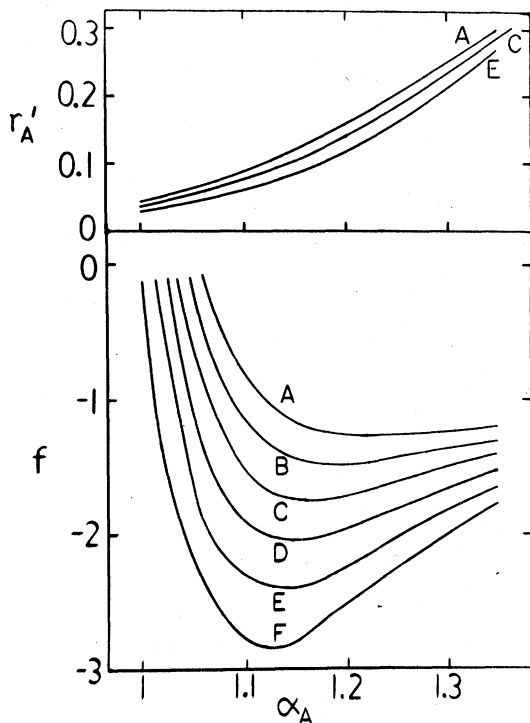


FIG. 3. Weighted rms amplitude r'_A (top diagram) and weighted configurational free energy f (lower diagram) vs average cell parameter α_A . The curves are designated A, B, C, D, E, F, for $T^* = 0.6, 0.5, 0.4, 0.3, 0.2,$ and 0.1 , respectively.

For six nearest neighbors, the self-consistent condition¹² is given by

$$3\alpha'^2 = r_A'^2 = \int \langle r^2 \rangle_\alpha p(\alpha) d\alpha = \int [r'(\alpha)]^2 p(\alpha) d\alpha, \quad (14)$$

where r'_A is the rms deviation from cell center weighted by the cell-size distribution.

An iteration procedure may now be used. For a given α_A , the initial value of $3\alpha'^2$ will be $[r'(\alpha_A)]^2$ from Fig. 2. Using Eq. (13) for $p(\alpha)$, a new value of $3\alpha'^2$ may be calculated from Eq. (14). The procedure is repeated (usually once or twice would be sufficient) until self-consistency is reached. The configurational free energy f per particle is

$$f(\alpha_A) = -T^*(\ln Q_N)/N = \int p(\alpha)\phi(\alpha) d\alpha, \quad (15)$$

with $\phi(\alpha)$ and $p(\alpha)$ given by Eqs. (9) and (13), respectively. That is, the free energy $\phi(\alpha)$ for a fixed cell size is now weighted by the cell-size distribution $p(\alpha)$. The results for r'_A and for f from Eqs. (14) and (15) are plotted versus α_A in Fig. 3 for several different temperatures. Although there is a general resemblance between Figs. 2 and 3, we note

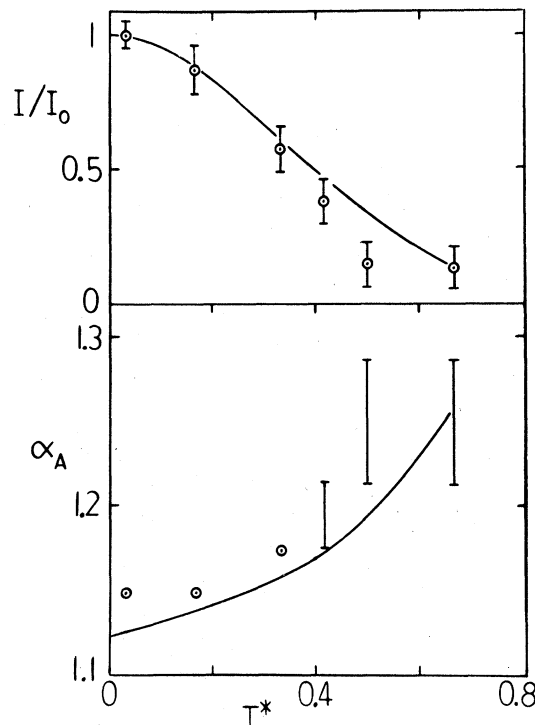


FIG. 4. Relative scattering intensity I/I_0 for the $\{10\}$ peak (top diagram) and average cell parameter α_A (lower diagram) vs reduced temperature T^* . The solid curves are theoretical results whereas the circles are neutron scattering data from Ref. 6.

that r'_A in Fig. 3 is somewhat larger (by approximately 10%) than r' in Fig. 2.

III. RESULTS

The most stable configuration would correspond to the free-energy minimum. From the minima of the free-energy curves in the lower diagram of Fig. 3 at various temperatures, the average cell parameter α_A is shown as a function of T^* in the lower diagram of Fig. 4. The calculated curve is in qualitative agreement with the experimental points of Taub *et al.*⁶ from neutron scattering studies of argon on Grafoil.

The calculated values of vibration amplitudes may also be compared with the relative intensities I/I_0 for the $\{10\}$ peaks of neutron scattering experiments where I and I_0 are the intensities at reduced temperatures T^* and 0, respectively. For a spatially random array of two-dimensional crystallites, the relative intensity is determined^{6,16} by both the Debye-Waller factor e^{-2W} and the correlation lengths L and L_0 at reduced temperatures T^* and 0

$$I/I_0 = e^{-2W}(L/L_0)^{1/2} \quad (16)$$

For two-dimensional lattices, the Debye-Waller fac-

tor e^{-2W} is related¹⁷⁻¹⁹ to the mean-square amplitude $\langle \mu^2 \rangle$ of vibration by

$$e^{-2W} = \exp\left(-\frac{1}{2}G^2\langle \mu^2 \rangle\right), \quad (17)$$

where $G = 2\pi/d$ and d is the spacing between adjacent lines of atoms. For the {10} peak, $d = \frac{1}{2}(\sqrt{3}\alpha_A)$. In the modified cell model, the mean-square amplitude of vibration (MSAV) of an argon atom from the cell center is $r_A'^2$ whereas the MSAV of the cell center itself is $\frac{1}{6}r_A'^2$ since the cell center is the center of mass of the six neighboring atoms. Hence we have

$$\langle \mu^2 \rangle = r_A'^2 + r_A'^2/6 = 7r_A'^2/6, \quad (18)$$

with r_A' given by Eq. (14) and plotted in Fig. 3.

In the upper diagram of Fig. 4, the relative intensity I/I_0 calculated from Eqs. (16) – (18) for the {10} peak is shown as the solid line. For these calculations, we have used the experimental values of correlation lengths⁶ from neutron scattering data. The experimental results⁶ for neutron scattering from argon adsorbed on Grafoil are shown as circles. The general agreement appears to be satisfactory.

IV. DISCUSSION

The original Lennard-Jones and Devonshire cell theory¹⁵ has assumed WS cells of identical shape (regular hexagons for two-dimensional lattices) and size. In the modified cell theory,¹² disordered structures have been introduced by using a self-consistent condition for the distribution of cell sizes. For the two-dimensional argon lattice, our calculated results appear to be in general agreement with the neutron scattering data of argon on Grafoil. If we omit the self-consistent condition and consider only cells of a fixed size, then the agreement would be less satisfactory and the calculated temperature dependence of the cell parameter would be considerably smaller than the experimental values.

Our results also indicate that the phase transitions for two- and three-dimensional argon lattices may be quite different. For the three-dimensional system,¹² The solid-liquid phase transition or the melting transition may be described in a very simple way. The configurational free energy f versus average cell parameter α_A curve at $T^* = 0.7$ has a rather flat minimum. At slightly lower and slightly higher temperatures, the minimum will shift abruptly toward smaller and larger cell sizes, respectively. For solid and liquid densities and for the melting temperature, there is general agreement between the calculated and experimental values. However, for two-dimensional systems, there is no longer any flat minimum for the f vs α_A curve at any temperature. From Fig. 3, we note that the curves for the $\alpha_A > 1.2$

region progressively became flatter at higher temperatures. For $T^* > 0.64$, the minimum may completely disappear, and the system may be identified as the "gas" phase. For argon on Grafoil, the argon atoms are nevertheless constrained by the argon-graphite interaction¹³ and do not move freely even in the gas phase. Due to the variations of argon-graphite potential across the substrate surface, certain epitaxial structures may be preferred at higher temperatures. Thus the phase transition for two-dimensional lattice of adsorbed argon atoms is not as sharp as the three-dimensional systems. Experimentally,^{20,21} rather broad specific-heat anomalies have been observed for rare gases (neon, argon, and krypton) on Grafoil and on xenon substrates. The temperatures corresponding to the specific-heat maxima appear to be proportional to the Lennard-Jones well depth ϵ , the reduced temperature T^* being approximately 0.56 in general agreement with our calculated value. In contrast to the three-dimensional system, there may not be any liquid phase and melting transition for the two-dimensional adsorbed argon layers.

The computer simulation results for hard-sphere systems have been recently reviewed by Barker and Henderson.²² For both two- and three-dimensional hard-sphere systems, phase transitions have been clearly observed between fluids at low densities and solids at high densities. Similar fluid-solid phase transitions have also been found for two-dimensional Lennard-Jones systems by Monte Carlo computer simulations.^{13,23-26} However, there is only fair agreement between various investigators on the transition temperature; the results ($T^* = 0.5-0.8$) are in general agreement with our calculations.

So far, we have only considered the idealized two-dimensional argon layer. However, for argon adsorbed on Grafoil surfaces, it is also necessary to consider the role of the periodic structure of the substrate in determining the cell size of the adsorbed layer. The graphite surface is composed of hexagons of carbon atoms, the nearest-neighbor C-C distance²⁷ being 1.42×10^{-8} cm. Hansen *et al.*¹³ have evaluated the lateral Ar-C potential at various lattice sites on the graphite surface and have found that the potential minimum is at the center of the carbon hexagon. If we consider the Ar-C potential only, then the potential energy per argon atom would be 0.1 lower for the commensurate argon lattice (with every argon atom located at the center of a carbon hexagon) as compared to the incommensurate lattice (random location of argon atoms with respect to the graphite lattice). For a commensurate lattice with structure very similar to the adsorbed argon layer, the cell parameter α_A would be three times the C-C distance in graphite; that is, $\alpha_A = 1.25$.

For a given temperature, the configurational free energies f per particle have been evaluated from Eq. (15) for the two-dimensional argon layer. We may

define $f_c = f(1.25)$ as the free energy for $\alpha_A = 1.25$ (the commensurate lattice) and f_m as the minimum free energy. On including the role of the substrate, we will now compare f_m with $f_c - 0.1$. At lower temperatures, $f_m < f_c - 0.1$, the cell parameter would correspond to the minimum free-energy state with incommensurate lattice. On the contrary, the commensurate lattice would be the stable configuration with lower free energy at higher temperatures. From Fig. 3, the transition temperature $T^* = 0.42$ may be determined from the condition $f_m = f_c - 0.1$. Experimentally, Taub *et al.*⁶ has found the cell parameter α_A to be 1.25 within experimental error for $T^* > 0.5$ and also that the argon lattice is incommensurate for $T^* < 0.41$. These experimental results are reproduced in Fig. 4 and are in good agreement with our

calculations.

In summary, a modified cell theory can be used to describe two-dimensional adsorbed argon layers on Grafoil, and the theoretical results are in general agreement with experimental data.

ACKNOWLEDGMENT

This work was partially supported by National Aeronautics and Space Administration under Grants No. NGR-09-011-057 and No. NSG-5186. These financial supports are gratefully acknowledged. We are grateful to Dr. L. Passell of Brookhaven National Laboratory and Dr. B. Mozer of National Bureau of Standards for helpful discussions.

- ¹J. J. Lander and J. Morrison, *Surf. Sci.* **6**, 1 (1967).
- ²P. W. Palmberg, *Surf. Sci.* **25**, 598 (1971).
- ³H. H. Farrell, M. Strongin, and J. M. Dickey, *Phys. Rev. B* **6**, 4703 (1972).
- ⁴J. Suzanne, J. P. Coulomb, and M. Bienfait, *Surf. Sci.* **40**, 414 (1973).
- ⁵H. Taub, L. Passell, J. K. Kjems, K. Carneiro, J. P. McTague, and J. G. Dash, *Phys. Rev. Lett.* **34**, 654 (1975).
- ⁶H. Taub, K. Carneiro, J. K. Kjems, L. Passell, and J. P. McTague, *Phys. Rev. B* **16**, 4551 (1977).
- ⁷J. K. Kjems, L. Passell, H. Taub, J. G. Dash, and A. D. Novaco, *Phys. Rev. B* **13**, 1446 (1976).
- ⁸K. Carneiro, W. D. Ellenson, K. Passell, J. P. McTague, and J. G. Dash, *Phys. Rev. Lett.* **34**, 654 (1975).
- ⁹J. P. McTague and M. Nielson, *Phys. Rev. Lett.* **37**, 596 (1976).
- ¹⁰C. Kittel, *Introduction to Solid State Physics*, 5th ed. (Wiley, New York, 1976), p. 12, Fig. 10(b).
- ¹¹J. O. Hirschfelder, C. F. Curtiss, and R. B. Bird, *Molecular Theory of Gas and Liquids* (Wiley, New York, 1954).
- ¹²T. Tsang and H. T. Tang, *Phys. Rev. A* **18**, 2315 (1978).
- ¹³F. E. Hanson, M. J. Mandell, and J. P. McTague, *J. Phys. (Paris)* **38**, C4-76 (1977).
- ¹⁴A. Rahman, *Phys. Rev.* **136**, A405 (1964).
- ¹⁵J. A. Barker, *Lattice Theories of the Liquid State* (Pergamon, Oxford, 1963).
- ¹⁶B. E. Warren, *Phys. Rev.* **59**, 693 (1941).
- ¹⁷C. Kittel, *Quantum Theory of Solids* (Wiley, New York, 1963), p. 379.
- ¹⁸A. A. Maradudin, E. W. Montroll, and G. H. Weiss, *Theory of Lattice Dynamics in the Harmonic Approximation* (Academic, New York, 1963), Chap. 7.
- ¹⁹C. Kittel, in Ref. 10, p. 64.
- ²⁰W. A. Steele and R. Karl, *J. Colloid Interface Sci.* **28**, 397 (1968).
- ²¹H. Cochrane, P. L. Walker, Jr., W. S. Diethorn, and H. C. Friedman, *J. Colloid Interface Sci.* **24**, 405 (1967).
- ²²J. A. Barker and D. J. Henderson, *Rev. Mod. Phys.* **48**, 587 (1976).
- ²³P. L. Fehder, *J. Chem. Phys.* **50**, 2617 (1969).
- ²⁴P. L. Fehder, *J. Chem. Phys.* **52**, 791 (1970).
- ²⁵R. M. J. Cotterill and L. B. Pederson, *Solid State Commun.* **10**, 439 (1972).
- ²⁶F. Tsien and J. P. Valletau, *Mol. Phys.* **27**, 177 (1974).
- ²⁷R. W. G. Wyckoff, *Crystal Structures*, 2nd ed. (Interscience, New York, 1964), Vol. 1, Chap. 2.